"Elevated heat pump" hypothesis for the aerosol-monsoon hydroclimate link: "Grounded" in observations?

The 'Elevated Heat Pump' Hypothesis for the Aerosol–Monsoon Hydroclimate Link: "Grounded" in Observations?

Sumant Nigam and Massimo Bollasina

Department of Atmospheric and Oceanic Science
University of Maryland, College Park, MD

Submitted to *J. Geophys. Res.* on December 31, 2009, revised March 2, 2010.

Corresponding author:
Sumant Nigam
Department of Atmospheric and Oceanic Science
3419 Computer and Space Science Building
University of Maryland, College Park, MD 20742-2425
E-mail: nigam@atmos.umd.edu

Abstract

The viability of the Elevated Heat Pump hypothesis – a mechanism proposed by Lau and Kim (2006) for absorbing aerosols' impact on South Asian summer monsoon hydroclimate – is assessed from a careful review of these authors' own analysis and others since then.

The lack of appreciation of the spatial distribution of the aerosol-related precipitation signal over the Indian subcontinent – its east-west asymmetric structure, in particular – apparently led to the development of this hypothesis. Its key elements have little observational support and the hypothesis is thus deemed untenable. Quite telling is the observation that local precipitation signal over the core aerosol region is negative, i.e., increased loadings are linked with suppressed precipitation, and not more as claimed by the hypothesis.

Finally, motivated by the need to address causality, Bollasina et al.'s (2008) analysis of contemporaneous aerosol-monsoon links is extended by examining the structure of hydroclimate lagged-regressions on aerosols. It is shown that findings obtained from contemporaneous analysis can be safely interpreted as representing the impact of aerosols on precipitation, not vice-versa. The possibility that both are shaped by a slowly-evolving, large-scale circulation pattern cannot however be ruled out.

1. Introduction

One of the areas of the world with high aerosol concentration is South Asia. The contribution of absorbing aerosols to the *long-term* change in summertime rainfall over the Indian subcontinent has been investigated by *Chung et al.* [2002], *Menon et al.* [2002], *Ramanathan et al.* [2005], *Chung and Ramanathan* [2006], *Lau et al.* [2006], *Meehl et al.* [2008], *Randles and Ramaswamy* [2008], *Collier and Zhang* [2009], and *Sud et al.* [2009]. The *interannual* variability of aerosol concentration and related summer monsoon rainfall variations has also been analyzed [e.g., *Lau and Kim,* 2006 (hereafter *LK06*); *Bollasina et al.,* 2008 (hereafter *BNL08*)].

Atmospheric general circulation models and observational analyses have both been deployed to understand aerosol-monsoon interaction. Modeling studies are insightful because of their ability to associate cause and effect in context of modeling experiments but some caution is necessary as model simulations are known to have significant biases in the climatological distribution and evolution of monsoon precipitation [e.g., *Dai*, 2006; *Bollasina and Nigam*, 2008]. Furthermore, aerosol effects are only partially represented in many models [e.g., *Kiehl,* 2007], often with large uncertainties [e.g., *Kinne et al.*, 2006]. It is expected that aerosols-clouds-precipitation processes and interactions will be greatly improved in the next generation of climate models [e.g., *Ghan and Schwartz,* 2007]. Observational studies, on the other hand, analyze a realistic system but characterization of the pertinent process sequence remains challenging on account of the myriad of feedbacks in the climate system. The influence of large-scale circulation on both aerosol distribution and regional hydroclimate also confounds efforts to elucidate the aerosol impact mechanisms [*Bollasina and Nigam*, 2009].

Several pathways have nonetheless been proposed for aerosol's influence on monsoon hydroclimate:

- Anomalous heating of air due to shortwave absorption by black carbon aerosols, which enhances regional ascending motions and thus precipitation in atmospheric general circulation models [*Menon et al.*, 2002; *Randles and Ramawamy*, 2008].

- Modulation of the summertime meridional sea surface temperature (SST) gradient in the Indian Ocean from reduced incidence of downward shortwave radiation in the northern basin in the preceding winter/spring. *Ramanathan et al.* [2005] and *Chung and Ramanathan* [2006] showed that aerosol-induced weakening of the SST gradient (leading to weaker summer monsoon rainfall) more than offsets the increase in summertime rainfall resulting from the "heating of air" effect in a coupled ocean-atmosphere model, leading to a net decrease in summer monsoon rainfall in the latter half of the 20^{th} century. The study of *Meehl et al.* [2008], also with a coupled model but with a more comprehensive treatment of aerosol-radiation interaction, supports Ramanathan et al.'s findings on the effect of black carbon aerosols on the Indian summer monsoon rainfall.

- Modulation of the meridional tropospheric temperature gradient from anomalous accumulation of absorbing aerosols against the southern slopes of the Himalayas in the pre-monsoon period. The elevated diabatic heating anomaly from aerosol absorption of shortwave radiation ("Elevated Heat Pump", hereafter EHP; *Lau et al.*, 2006; *LK06*) over the southern slopes of the Tibetan plateau in April-May reinforces the climatological meridional temperature gradient and leads to monsoon intensification in June-July in this scheme.

- Anomalous heating of the land-surface by aerosol-induced reduction in cloudiness (the "semi-direct" effect) and the attendant increase in downward surface shortwave radiation. Stronger heating of the land-surface in May generates greater ocean-atmosphere contrast and thus more monsoon rainfall in June in this posited mechanism [*Bollasina et al.*, 2008]. The

105 importance and potential impacts of aerosol-land–atmosphere interactions on the Indian
106 monsoon have been summarized by *Niyogi et al.* [2007] and *Pielke et al.* [2007].

107 It is interesting that none of the mechanisms except the last one consider aerosol effects on
108 cloudiness (other than those due to attendant heating and circulation changes). The first three
109 pathways are primarily rooted in the aerosol's direct effect on shortwave radiation: tropospheric
110 absorption and surface dimming over both land and ocean. The impact on cloudiness can,
111 perhaps, be neglected in winter when the central and northern Indian subcontinent is relatively
112 cloud-free, but not in late spring and summer when cloudiness tracks monsoon development.
113 Climate models are still ill-equipped in dealing with the complexities of aerosol-cloud interaction
114 (reckoned important in summer) and can thus provide limited insight on the net effect of aerosols
115 on *summer* monsoon hydroclimate and the related impact mechanisms. The indirect effect is not
116 well understood and thus inadequately represented. As for the semi-direct effect, it is likely
117 underrepresented due to uncertainties in aerosol distribution and optical properties, and potential
118 misrepresentation of related cloud responses.

119 A key objective of the present study is to examine the viability of the interesting EHP
120 mechanism. LK06 investigated the link between absorbing aerosols and summer monsoon
121 rainfall and circulation in an observational analysis, targeting the effects of the pre-monsoon
122 aerosol loading over the Indo-Gangetic Basin (IGB). Using composite and regression analysis
123 keyed to the TOMS Aerosol Index (AI) averaged over the IGB, the authors posit that piling up of
124 absorbing aerosols (i.e., dust and black-carbon) along the Himalayan foothills and southern
125 slopes of the Tibetan Plateau during April-May leads to diabatic heating of the lower-to-mid
126 troposphere from aerosol absorption of solar radiation. The heated air over the southern slopes of
127 the Tibetan Plateau rises, drawing warm and moist low-level inflow from the northern Indian

Ocean. Aerosol extinction (due to absorption and scattering) of solar radiation – the "solar dimming" effect – is moreover reckoned to produce surface cooling over central India, with the resulting increased stability leading to rainfall suppression there. A large-scale response, including a regional meridional overturning circulation with rising motion (and increased rainfall) in the Himalayan foothills and northern India and sinking motion over the northern Indian Ocean, is then envisioned (see Section 2 in *LK06* for more discussion). The EHP hypothesis has recently motivated a NASA field campaign involving ground and remote observations in the IGB and Himalayan-Tibetan regions.

A careful review of *LK06* and other analyses since then [*BNL08*; *Gautam et al.*, 2009] however reveals that the EHP hypothesis is not grounded in observations. The study of *BNL08*, observationally based and similar to *LK06* in many respects, indicates in particular that the EHP mechanism is rooted in the *expansive* zonal averaging employed in *LK06*. Such overly-wide averaging is without basis since the western and eastern sectors of the averaged region have oppositely signed hydroclimate signals, leading to spurious collocation of aerosol loading (concentrated in the western sector) and the dominating hydroclimate signal (of the eastern sector). The EHP hypothesis has other difficulties as well, all discussed below.

Another objective of this study is to extend *BNL08*'s analysis of aerosol-monsoon links which emphasized the aerosol semi-direct effect and attendant *heating* of the land surface. The EHP hypothesis, in contrast, highlights the direct effect of aerosols and related *cooling* (heating) of the land surface (atmosphere). *BNL08*'s contemporaneous analysis for late-spring is complemented here by displaying the aerosol-monsoon links with aerosol leading, which provide further insights into cause and effect, albeit cursorily in view of the monthly analysis resolution. The article is organized as follows: Section 2 articulates the perceived difficulties with the EHP

hypothesis vis-à-vis observations, while Section 3 presents key results from the analysis of aerosol-monsoon links. Concluding remarks follow in Section 4.

2. Difficulties with the EHP hypothesis

To critique the observational basis for the EHP hypothesis, we first reproduced *LK06* analysis before assessing its sensitivity to some attributes. The EHP hypothesis lacks observational support in our opinion for the following reasons:

- *LK06*, unfortunately, did not show the IGB AI-related precipitation footprint in May when aerosol concentration is at its peak. The lack of appreciation of the precipitation distribution – primarily zonal, with decreased rainfall over western-central India (where aerosol is concentrated) and increased rainfall over northern Burma and the far eastern Indian state of Assam (Fig. 1a)[1] – must have allowed *LK06* to entertain EHP-type notions, we surmise. Had the authors realized that the IGB AI rainfall regressions in the aerosol-loading region which includes Himalayan foothills (Box-I in *LK06*'s Fig. 1b; green-sided rectangle in Fig. 1a here) are weak and that too of opposite sign (i.e., rainfall reduction) in May, they may have shied away from proposing the EHP hypothesis[2]. The May rainfall signal of a more geographically focused AI time series (defined by solid dots in Fig. 1 of *BNL08*) is also very weak in the Himalayan foothills and northeastern India, with rainfall suppression again indicated (Fig. 3 of *BNL08*).

[1] Figure 1 shows the May regressions /correlations on the May IGB AI. The May index was chosen for consistency with BNL08 but one could have as well chosen the April-May average IGB AI to be fully consistent with LK06. The May precipitation regressions on the latter are indistinguishable from those in Fig. 1a.

[2] The EHP signal should be manifest in the monthly average as the contributing processes operate on shorter time scales.

- A figure that plays a key role in the formulation of the EHP hypothesis is Fig. 2 in *LK06*: Panels 2a and 2b depict the monthly evolution of sector-averaged aerosol and precipitation anomalies as a function of latitude. The anomalies are from composites keyed to the IGB AI. Based on this figure – misleading for reasons discussed next – *LK06* (Section 3.2) conclude that "*At the time of the maximum build up of aerosol in May, rainfall is increased over northern India (20°–28°N) but reduced over central India (15°–20°N). The rainfall pattern indicates an advance of rainy season over northern India starting in May, followed by increased rainfall over all-India from June to July, and decreased rainfall in August.*" This incorrectly drawn conclusion is the backbone of the EHP hypothesis. Panel 2b, in particular, is misleading in context of this hypothesis because an overly-wide longitudinal sector average (65°-95°E) is displayed (the sector is marked in yellow in Fig. 1a). Such extensive averaging is misleading as it suggests spatial collocation of aerosol loading and enhanced precipitation, when, in fact, there is little overlap among them: Precipitation is enhanced in the very narrow sector to the far right (90°-95°E), and not at all in region I (70°-90°E); see Fig. 1a. A similar reasoning can be applied to Fig. 3a in *LK06*: Enhanced meridional motion and subsequent upward velocity are actually observed only eastward of 90°E (Fig. 1f of the present work), which is a very narrow band compared to the range of longitudes included in the average. Figures 2b and 3a in *LK06* thus do not provide observational evidence for the EHP hypothesis, contrary to claims. Examination of the IGB AI-related May precipitation anomaly (Fig. 1a) shows clearly that rainfall does not increase over Northern India (where aerosol loadings are largest); it is, in fact, suppressed. *LK06* obtain a precipitation increase only because their overly-wide averaging masks the suppressed precipitation over North India favoring the large precipitation increase farther to the east.

- The EHP hypothesis is predicated on the piling up of absorbing aerosols against the southern slopes of the Himalayas and over southern Tibetan plateau. The core of the May aerosol standard deviation is however located not over elevated terrain but well south of the Himalayan range (Fig. 1b in *BNL08* and Fig. 1b in *LK06*).

- An important element of the EHP hypothesis is the diabatic heating of the troposphere above elevated terrain. Citing *Gautam et al.* [2009], *"According to the EHP hypothesis, aerosol forcing resulting from absorption of solar radiation due to enhanced build-up of dust aerosols in May, mixed with soot from industrial/urban pollution over the IGP, may cause strong convection and updrafts in the middle-upper troposphere resulting in positive tropospheric temperature anomalies northward, most pronounced over the southern slopes of the TP and the Himalayas [Lau et al., 2006; Lau and Kim, 2006]."* The AI-related tropospheric (1000-300 hPa layer-average) warming (Fig. 4a in *LK06*) is, of course, not evidence of this (although it is taken as such in *Gautam et al.,* 2009) as the displayed warming signal lags AI by one month in the *LK06* figure. The IGB-AI related contemporaneous (May) warming in the lower (surface-700 hPa) and upper troposphere (700-300 hPa) is shown in Figs. 1b-c, respectively. Correlation analysis shows only the former to be significant. In neither case, however, positive temperature anomalies are found northward of the core aerosol loading region, and certainly not above the 700 hPa level. As discussed later, the lower tropospheric warming arises from the warming of the land-surface, as evident from the vertical structure of the AI-related temperature signal (Fig. 7 in *BNL08*).

- The EHP hypothesis posits that rainfall enhancement is confined to the foothill region because aerosol induced "solar dimming" leads to the cooling of the Indo-Gangetic Plains, limiting convective instability. There is no evidence for this in observations. To the contrary,

the AI-related downward shortwave radiation anomaly (Fig. 1d)[3] is positive over much of the subcontinent, leading to a warmer land-surface. Other factors, e.g., advection may contribute as well. The associated 2-m temperature anomaly (Fig. 1e) reflects the modulation of insolation. The "solar dimming" feature of the EHP hypothesis was perplexing to begin with, as detection of "solar dimming" is far more challenging in late spring and early summer when cloudiness variations can be confounding. Observational evidence shows an unambiguous warming of the land surface in May when aerosol loading is anomalously high, attesting to the dominance of the aerosol semi-direct effect (or decreased cloud cover) over any "solar dimming" due to aerosol extinction.

- Recently, *Gautam et al.* [2009] have correlated the lower and upper tropospheric temperature anomalies over Northern India in March-May with the concurrent AI over the region (their Fig. 3), finding significant correlations (~0.65). This correspondence however cannot be considered evidence for the EHP hypothesis any more than it can for the aerosol semi-direct effect. As discussed above (and in Fig. 9 of *BNL08*), the AI-related signal in downward surface shortwave radiation is positive over the subcontinent, leading to surface (and lower tropospheric) warming, providing forceful evidence for the dominance of the semi-direct effect.

- The non-collocation of the aerosol loading and rainfall enhancement regions in May is concerning in context of the EHP hypothesis, as noted above. A more reasonable and straightforward explanation for increased rainfall over northeastern India is orographic uplift

[3] The downward surface shortwave radiation is from the International Satellite Cloud Climatology Project (ISCCP) FD SRF data set [*Zhang et al.,* 2004]. The field is generated by NASA's Goddard Institute of Space Studies (GISS) general circulation model using ISCCP cloud fields and the GISS aerosol climatology. As shown in Fig. 9 in BNL08, this analysis of surface shortwave radiation compares favorably with the Global Energy and Water Cycle Experiment's (GEWEX) SRB diagnosis [*Gupta et al.,* 1999].

of the moisture laden air from the Bay of Bengal. The southerly flow is generated as part of the anomalous low-level cyclonic circulation (Fig. 1f), anchored by land-surface heating (Figs. 1e, 1b) and resulting low pressure over the subcontinent. [More generally, the aerosol loading and rainfall enhancement/suppression regions need not be collocated as the aerosol impact is often generated from induced regional circulation anomalies.]

The EHP hypothesis is not without conceptual difficulties as well: For instance, if aerosol-induced rising motions were to lead to *local* rainfall enhancement in the foothill region, aerosol washout would rapidly occur. The EHP would then serve as an *aerosol self-limiting mechanism* in the Himalayan foothills, limiting its efficacy in impacting summer monsoon evolution over the larger subcontinent.

3. Aerosol-leading hydroclimate links

The contemporaneous analysis of aerosol-monsoon hydroclimate links for May reported in *BNL08* precludes attribution of cause and effect. One interpretation of the findings, as discussed in section 5 of that paper, could have been that aerosol loading responds to concurrent rainfall variations due to washout effect, which is not an unreasonable proposition. This possibility was however ruled out in *BNL08* by additional analysis in which the April AI over the Indo-Gangetic Plain (IGP) was regressed on May and June's precipitation and circulation. Although discussed to some extent, the lagged regression patterns were not displayed in *BNL08*, leading to some lingering concerns on causality.

Monthly lagged regressions on the IGP aerosol index (defined as in *BNL08*) can be insightful provided that the AI itself is autocorrelated on time scales longer than a month. Figure 1f in

BNL08 shows the autocorrelation structure of both April and May indices. The indices are significantly correlated (~0.6), indicating anomaly persistence longer than one month. Figure 2 in *BNL08* provides context for the multi-month timescale by showing how 'aerosol events' over the Indo-Gangetic Plain can be generated in the pre-monsoon period from advection of dust and pollutants by the prevailing low-level westerlies, i.e., by a process other than local precipitation which operates on much shorter time scales.

The contemporaneous and lagged precipitation regressions on the April IGP AI are shown in Fig. 2 (a-c). Close comparison with Fig 3 in *BNL08* (top row; contouring and shading intervals are identical) indicates striking similarity between the contemporaneous and one-month aerosol-leading regressions of May precipitation [*BNL08*'s Fig. 3 (top-left panel) and Fig. 2b, respectively]. The east-west asymmetry, in particular, is well captured in the aerosol-leading regressions. The similarity extends to the June precipitation patterns: the 2-month lagged regressions on the April AI and the 1-month lagged regressions on the May AI. The April and May IGP AI regressions of the May 2-m air temperature also exhibit notable similarity [Fig. 2d-e and *BNL08*'s Fig 8 (top-left), respectively], indicating coherent development of surface warming and the dominance of the aerosol semi-direct effect over the direct one.

The extensive similarity between the aerosol-leading and contemporaneous regressions of precipitation along with evidence for the multi-month duration of aerosol episodes in the pre-monsoon onset period should address the causality issue. The findings of *BNL08* obtained from contemporaneous analysis thus represent the impact of aerosols on precipitation, not vice-versa.

4. Concluding Remarks

The study seeks to ascertain the viability of the EHP hypothesis – a mechanism proposed by *LK06* for absorbing aerosols' impact on South Asian summer monsoon hydroclimate. A careful review of *LK06*'s analysis and others since then [*Bollasina et al.*, 2008; *Gautam et al.,* 2009] reveals that the EHP hypothesis is not grounded in observations. A lack of appreciation of the spatial distribution of the aerosol-related May precipitation signal over the Indian subcontinent – its east-west asymmetric structure, in particular – as reflected in gross zonal-averaging (65°-95°E) of the signal in *LK06* (Fig. 2b) led to this hypothesis.

We show that key elements of the EHP hypothesis have no basis in observations and the hypothesis is thus deemed untenable:

- The core of the May aerosol standard deviation is located not over the southern Himalayan slopes or elevated terrain but southward over the northern Indo-Gangetic Plain.

- Aerosol-related downward surface shortwave radiation and 2-m air temperature signals are positive over the core region and the northern subcontinent, i.e., increased loadings are associated with more surface insolation and a warmer land surface (not a colder one, as per EHP hypothesis). This indicates the dominance of the aerosol semi-direct effect over the direct one (solar dimming).

- More importantly, the concurrent local precipitation signal over the core aerosol region in May is negative, i.e., increased loadings are linked with suppressed precipitation (not more, as claimed by the EHP hypothesis).

- Aerosol-related tropospheric warming is confined to the lower troposphere. Sensible heating from the land-surface is, perhaps, most important (see Fig. 8 in BNL08).

- The EHP hypothesis has a self-limiting element: If aerosol-induced rising motions were to lead to local rainfall enhancement in the foothill regions, as claimed, aerosol washout would occur, limiting its intensity and large-scale influence.

- The EHP hypothesis can perhaps be mimicked by atmospheric models but this cannot be an indication of its relevance in nature as the representation of aerosol indirect and semi-direct effects in models mentioned above is primitive. Observational analysis is, of course, not without its own uncertainties.

Finally, we extend the analysis of contemporaneous aerosol-monsoon links reported in *BNL08* by examining the structure of the one- and two-month aerosol-leading regressions on hydroclimate. The extension is motivated by the need to address causality. The extensive similarity between the aerosol-leading and contemporaneous regressions on precipitation along with evidence for the multi-month duration of aerosol episodes in the pre-monsoon period suggest that the *BNL08* findings obtained from contemporaneous analysis represent the impact of aerosols on precipitation, not vice-versa.

The possibility that both aerosol and precipitation anomalies, in turn, are shaped by a slowly evolving, large-scale circulation pattern cannot presently be ruled out, in part because current atmospheric models and observational analyses are unable to tease apart regional feedbacks from the large-scale influence. Some caution is thus warranted in the interpretation of aerosol mechanisms, as further discussed in *Bollasina and Nigam* [2009].

322 *Acknowledgements:* The authors acknowledge NSF support through ATM-0649666 and DOE
323 support through DEFG0208ER64548 and DESC0001660 grants. The authors gratefully
324 acknowledge two very constructive and insightful reviews.
325

References

Bollasina, M., and S. Nigam (2009), Absorbing aerosols and pre-summer monsoon hydroclimate variability over the Indian subcontinent: The challenge in investigating links, *Atmos. Res., 94,* 338-344.

Bollasina, M., S. Nigam, and K.-M. Lau (2008), Absorbing aerosols and summer monsoon evolution over South Asia: An Observational Portrayal, *J. Clim., 21,* 3221-3239.

Bollasina, M., and S. Nigam (2008), Indian Ocean SST, evaporation, and precipitation during the South Asian summer monsoon in IPCC-AR4 coupled simulations, *Clim. Dyn.* doi:10.1007/s00382-008-0477-4.

Chung, C. E., and V. Ramanathan (2006), Weakening of North Indian SST gradients and the monsoon rainfall in India and the Sahel, *J. Climate, 19*, 2036-2045.

Chung, C. E., V. Ramanathan, and J. T. Kiehl (2002), Effects of the South Asian absorbing haze on the northeast monsoon and surface-air exchange, *J. Climate, 15*, 2462- 2476.

Collier, J. C., and G. J. Zhang (2009), Aerosol direct forcing of the summer Indian monsoon as simulated by the NCAR CAM3, *Clim. Dyn., 32,* 313–332, doi:10.1007/s00382-008-0464-9.

Dai, A., (2006), Precipitation characteristics in eighteen coupled climate models, *J. Climate, 19*, 4605-4630.

Gautam, R., N. C. Hsu, K. ‐ M. Lau, S. ‐ C. Tsay, and M. Kafatos (2009), Enhanced pre-monsoon warming over the Himalayan-Gangetic region from 1979 to 2007, *Geophys. Res. Lett., 36,* L07704, doi:10.1029/2009GL037641.

Ghan, S. J., and S. E. Schwartz (2007), Aerosol properties and processes: A path from field and laboratory measurements to global climate models, *Bull. Amer. Meteor. Soc., 88,* 1059–1083.

348 Gupta, S. K., N. A. Ritchey, A. C. Wilber, C. H. Whitlock, G. G. Gibson, and P. W. Stackhouse
349 (1999), A climatology of surface radiation budget derived from satellite data. *J. Climate*, *12,*
350 2691-2710.
351 Kiehl, J. T. (2007), Twentieth century climate model response and climate sensitivity, *Geophys.*
352 *Res. Lett., 34*, L22710, doi:10.1029/2007GL031383.
353 Kinne, S., and Coauthors (2006), An AeroCom initial assessment optical properties in aerosol
354 component modules of global models, *Atmos. Chem. Phys*., *6*, 1815-1834.
355 Lau, K.-M., and K.-M. Kim (2006), Observational relationships between aerosol and Asian
356 monsoon rainfall, and circulation, *Geophys. Res. Lett.*, *33*, L21810,
357 doi:10.1029/2006GL027546.
358 Lau, K.-M., M. K. Kim, and K.-M. Kim (2006), Aerosol induced anomalies in the Asian summer
359 monsoon- the role of the Tibetan Plateau, *Clim. Dyn.*, *26*, 855-864, doi:10.1007/s00382-006-
360 0114-z.
361 Meehl, G. A., J. M. Arblaster, and W. D. Collins (2007), Effects of black carbon aerosols on the
362 Indian monsoon, *J. Climate*, *21*, 2869-2882.
363 Menon, S., J. Hansen, L. Nazarenko, and Y. Luo (2002), Climate effects of black carbon aerosols
364 in China and India, *Science*, *297*, 2250-2253.
365 Niyogi, D., H.-I. Chang, F. Chen, L. Gu, A. Kumar, S. Menon, R. A. Pielke (2007), Potential
366 impacts of aerosol–land–atmosphere interactions on the Indian monsoonal rainfall
367 characteristic, *Nat. Hazards, 42,* 345-359.
368 Pielke Sr., R. A., J. O. Adegoke, T. N. Chase, C. H. Marshall, T. Matsui, and D. Niyogi (2007),
369 A new paradigm for assessing the role of agriculture in the climate system and in climate
370 change, *Agric. Forest Meteor., Special Issue, 132,* 234-254.

371 Ramanathan, V., and Coauthors (2005), Atmospheric Brown Clouds: Impacts on South Asian
372 Climate and Hydrological Cycle. *PNAS*, *102*, 5326-5333.
373 Randles, C. A., and V. Ramaswamy (2008), Absorbing aerosols over Asia: A Geophysical Fluid
374 Dynamics Laboratory general circulation model sensitivity study of model response to
375 aerosol optical depth and aerosol absorption, *J. Geophys. Res., 113*, D21203,
376 doi:10.1029/2008JD010140.
377 Sud, Y. C., and Coauthors (2009), Sensitivity of boreal-summer circulation and precipitation to
378 atmospheric aerosols in selected regions – Part 1: Africa and India, *Ann. Geophys., 27*, 3989-
379 4007.
380 Zhang, Y., W. B. Rossow, A. A. Lacis, V. Oinas, and M. I. Mishchenko (2004), Calculation of
381 radiative fluxes from the surface to top of atmosphere based on ISCCP and other global data
382 sets: Refinements of the radiative transfer model and the input data, *J. Geophys. Res.*, *109*,
383 D19105, doi:10.1029/2003JD004457.
384
385

Figure Captions

Figure 1. May regressions (shaded, with the grey line indicating the zero contour) and correlations (black contours) on the TOMS AI time series averaged over the area (70°-90°E, 22.5°-30°N, green rectangle in (a); the Box-I domain in LK06) of: (a) precipitation (mm day^{-1}, from the Global Precipitation Climatology Project, GPCP); (b) surface-700 hPa average temperature (°C, from the ECMWF Reanalysis, ERA-40); (c) 700-300 hPa average temperature (°C, from ERA-40); (d) downward shortwave radiation at the surface (0.1×W m^{-2}, from the ISCCP FD dataset), (e) 2-m air temperature (°C, from ERA-40), (f) moisture flux (Kg m^{-1} s^{-1}; vectors, values below 20 Kg m^{-1} s^{-1} have been masked out) and its convergence (Kg m^{-2} s^{-1}; shaded, positive values representing convergence) mass-weighted and vertically integrated between the surface and 850 hPa. The time series were not detrended before computing the correlations, to closely compare with maps in LK06. Data are for the period 1979-1992, except radiation which is only available from 1984. Correlations are only shown in terms of the 95% and 99% significance levels (±0.53 (±0.67) and ±0.66 (±0.79), respectively). Inconsistency in the AI time series after 1992 restricted the correlations to the 14-year period considered here. Green and yellow rectangles in Fig. 1a denote the regions (70°-90°E, 22.5°-30°N and 65°-95°E, 22.5°-30°N, respectively) used by LK06 to define the AI time series (their Fig. 1c) and for displaying cross-sections of composite anomalies (their Figs. 2b and 3), respectively.

Figure 2. *Top panels:* GPCP precipitation (mm day^{-1}) regressed on the April TOMS AI time series (averaged over the same points highlighted in Fig. 1a of BNL08) for (a) April, (b) May, and (c) June. The ±0.53 contour line shows the 95% confidence level. *Bottom panels:* 2-m air temperature (T2M, °C; data from ERA-40) regressed on the April AI time series for (d) May and (e) June (the ±0.46 contour line show the 90% confidence level). Data are for the period 1979-1992. Both data were detrended before computing the regressions.

Figures

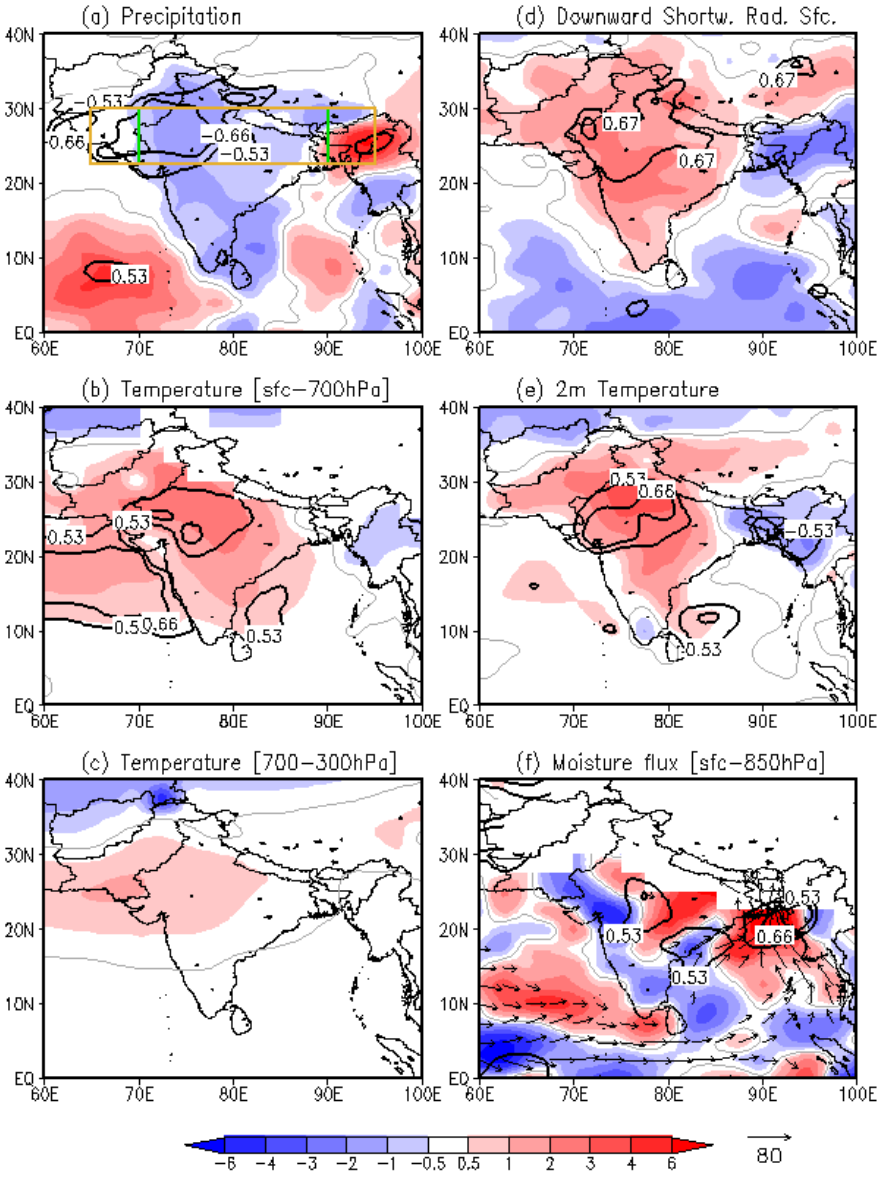

Figure 1. May regressions (shaded, with the grey line indicating the zero contour) and correlations (black contours) on the TOMS AI time series averaged over the area (70°-90°E, 22.5°-30°N, green rectangle in (a); the Box-I domain in LK06) of: (a) precipitation (mm day^{-1}, from the Global Precipitation Climatology Project, GPCP); (b) surface-700 hPa average temperature (°C, from the ECMWF Reanalysis, ERA-40); (c) 700-300 hPa average temperature (°C, from ERA-40); (d) downward shortwave radiation at the surface (0.1×W m^{-2}, from the ISCCP FD dataset), (e) 2-m air temperature (°C, from ERA-40), (f) moisture flux (Kg m^{-1} s^{-1}; vectors, values below 20 Kg m^{-1} s^{-1} have been masked out) and its convergence (Kg m^{-2} s^{-1}; shaded, positive values representing convergence) mass-weighted and vertically integrated between the surface and 850 hPa. The time series were not detrended before computing the correlations, to closely compare with maps in LK06. Data are for the period 1979-1992, except radiation which is only available from 1984. Correlations are only shown in terms of the 95% and 99% significance levels (±0.53 (±0.67) and ±0.66 (±0.79), respectively). Inconsistency in the AI time series after 1992 restricted the correlations to the 14-year period considered here. Green and yellow rectangles in Fig. 1a denote the regions (70°-90°E, 22.5°-30°N and 65°-95°E, 22.5°-30°N, respectively) used by LK06 to define the AI time series (their Fig. 1c) and for displaying cross-sections of composite anomalies (their Figs. 2b and 3), respectively.

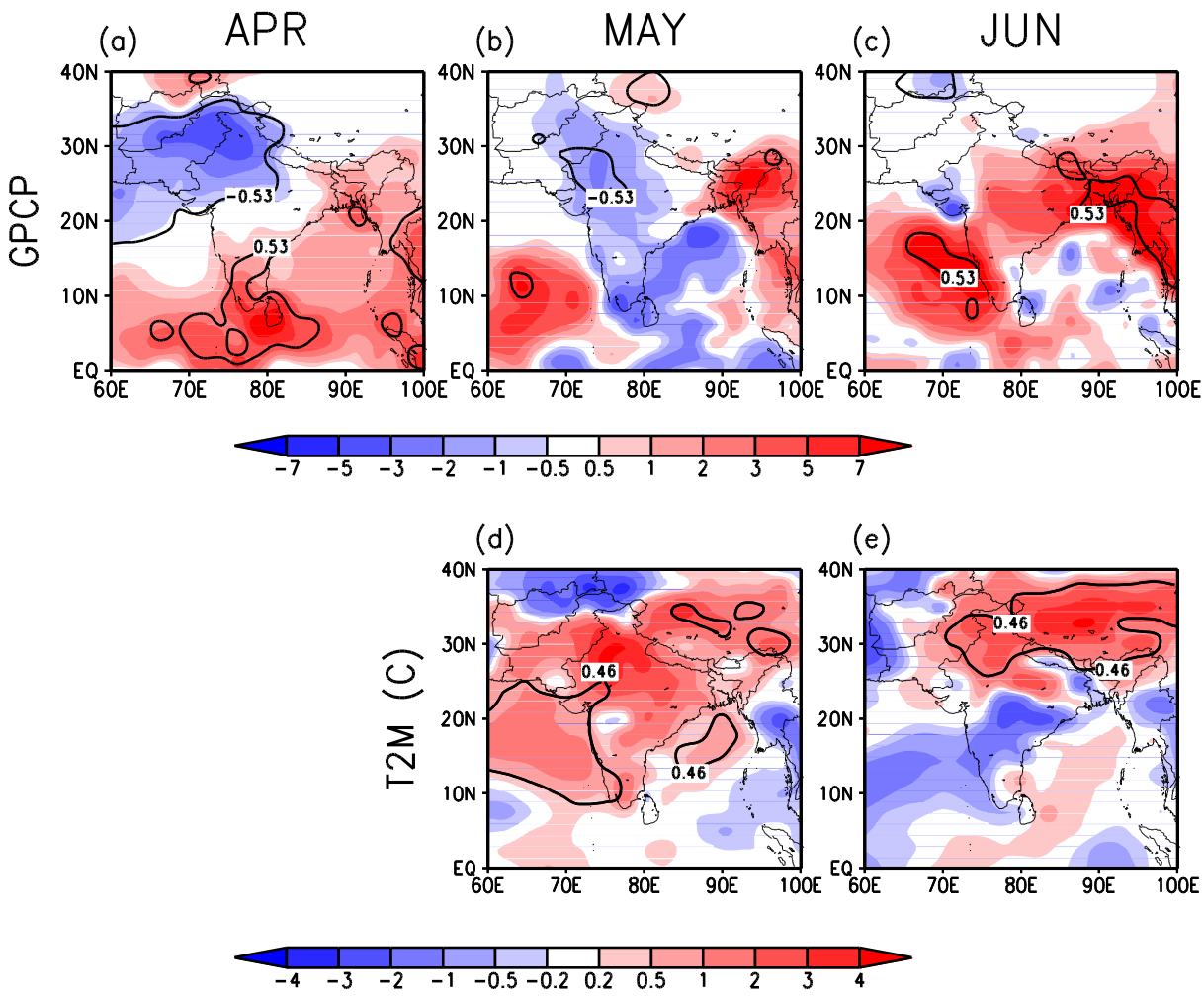

Figure 2. *Top panels:* GPCP precipitation (mm day^{-1}) regressed on the April TOMS AI time series (averaged over the same points highlighted in Fig. 1a of BNL08) for (a) April, (b) May, and (c) June. The ±0.53 contour line shows the 95% confidence level. *Bottom panels:* 2-m air temperature (T2M, °C; data from ERA-40) regressed on the April AI time series for (d) May and (e) June (the ±0.46 contour line show the 90% confidence level). Data are for the period 1979-1992. Both data were detrended before computing the regressions.